Polymer Chemistry

ROYAL SOCIETY OF CHEMISTRY

PAPER

View Article Online
View Journal | View Issue

Cite this: *Polym. Chem.*, 2023, **14**, 3364

Molecular-level insight into the low-*k* properties and regulatory mechanisms of polybenzoxazines†

Manlin Yuan,[a] Xin Lu,[a] Shiao-Wei Kuo [b] and Zhong Xin *[a]

Received 19th May 2023,
Accepted 20th June 2023

DOI: 10.1039/d3py00556a

rsc.li/polymers

The increasing demand for high signal transmission speed and low loss is attracting research efforts to design low dielectric constant (low-*k*) polymers. In this paper, a novel cyclohexyl-containing main-chain benzoxazine BZ-aptmds was prepared. 4-Cyclohexylphenol was employed as a capping agent to react with the polar groups at the end of the chain and control the molecular weight of polybenzoxazine. Then, a polybenzoxazine named PCBZ-aptmds with a low dielectric constant (2.62), low dielectric loss (0.0042), low water absorption, and good thermal properties was prepared. To deeply explore the effect mechanism of polybenzoxazines, molecular models were established according to density functional theory and molecular dynamics simulation. The volume polarizability and proportion of non-polar domains simulated from molecular-level insight have an excellent correlation with the experimental dielectric constant. In particular, the theoretically calculated values of the dielectric constant of three polybenzoxazines are in good agreement with the experimental results.

1. Introduction

The rapid expansion of electronic communication has brought significant attention to the requirements for signal transmission speed and loss, which are closely related to the dielectric constant and loss of dielectric materials.[1–4] Polybenzoxazines are a type of promising material with intrinsic low dielectric constant (low-*k*), high flame retardancy, great adhesion, good oxidation resistance, and superior hydrophobicity.[5–9] Benzoxazine monomers are synthesized from phenols, primary amines, and formaldehyde *via* Mannich condensation.[10] The diversity of raw materials endows polybenzoxazines with flexible molecular design properties. Taking advantage of this feature, polybenzoxazines with special groups can be designed flexibly according to their end applications. Benzoxazole, *tert*-butyl, alicyclic rings, and long alkyl chains have been applied to the molecular design of low-*k* polybenzoxazine according to the theoretical guidance of reducing molecular polarizability and dipole density.[11–15] Among them, alicyclic rings can effectively reduce the dielectric constant of polymers due to their small isotropic polarizability tensors.[16] The rigid alicyclic ring can also prevent molecular stacking and increase the free volume of polymers.[17] In addition, the C–C bonds in alicyclic rings have superior hydrophobicity, which is conducive to reducing the water absorption of polymers. Therefore, the introduction of aliphatic rings into the molecular structure is an efficient method to prepare low-*k* polybenzoxazines.

Although many studies successfully prepared various polybenzoxazines with relatively low dielectric constants, the regulatory mechanism of the molecular structure on dielectric properties is still unclear. In recent years, molecular simulation has become increasingly important in guiding the design and development of high-performance materials.[18,19] Density functional theory (DFT) can quantitatively simulate the polarizability, dipole moment, and electrostatic potential distribution of repeated segments of polymers, which are closely related to dielectric properties,[20–22] while molecular dynamics (MD) simulation can calculate the number density and chain mobility of polymers on a larger scale.[23,24] The dielectric constant of polymers can be simulated by combining DFT and MD, and the results are in high agreement with the experimental values.[23,25,26]

In this work, three novel cyclohexyl-containing benzoxazines were designed and synthesized using 4-cyclohexylphenol, 4,4′-cyclohexylidenebisphenol and 1,3-bis(aminopropyl)tetramethyl disiloxane. As the capping agent, 4-cyclohexylphenol can react with polar amino groups at the chain end of main-chain benzoxazine BZ-aptmds and control the molecular weight. Then, the hydrophobicity, thermal properties, and dielectric properties of the three polybenzoxazines were tested. Three amorphous boxes of polybenzoxazine were established by combining MD and DFT (Fig. 1), and their parameters such

[a]*School of Chemistry Engineering, East China University of Science and Technology, Shanghai, 200237, People's Republic of China. E-mail: xzh@ecust.edu.cn*
[b]*Department of Materials and Optoelectronic Science, Nation Sun Yat-Sun University, Kaohsiung, 80424, Taiwan*

† Electronic supplementary information (ESI) available. See DOI: https://doi.org/10.1039/d3py00556a

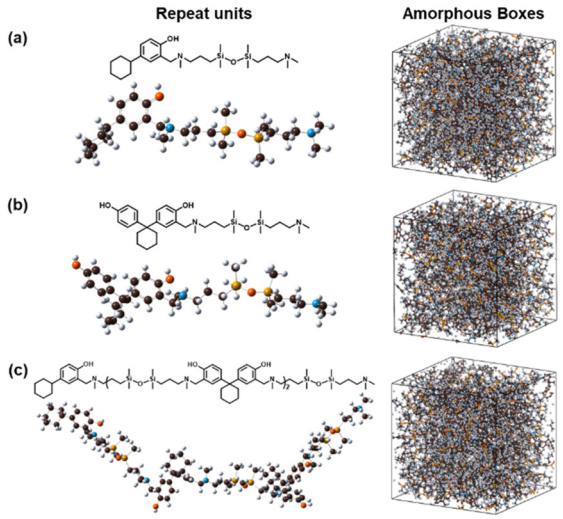

Fig. 1 Repeat units for DFT simulation and amorphous boxes for MD simulation of (a) PC-aptmds, (b) PBZ-aptmds, and (c) PCBZ-aptmds.

as polarizability, van der Waals volume, and mean square displacement were simulated from molecular-level insight. Furthermore, the calculated values of the dielectric constant of the three polybenzoxazines are in superior agreement with the experimental values.

2. Results and discussion

2.1 Synthesis and characterization of benzoxazine prepolymers

Three cyclohexyl-containing benzoxazine prepolymers C-aptmds, BZ-aptmds, and CBZ-aptmds were designed and synthesized using the strategy of reducing molecular polarizability, as shown in Fig. 2a. FT-IR was employed to confirm the molecular structures of the three benzoxazine prepolymers, and the results are shown in Fig. 2b. The absorption peaks of the oxazine rings in the three benzoxazine prepolymers are almost identical because of the structural similarity. The characteristic absorption peaks of the oxazine ring at 1321, 1231, 1147, 941, and 923 cm^{-1} were observed, which represent CH_2 wagging, C–O–C stretching vibration, C–N–C stretching vibration, and oxazine ring vibration, respectively. The spectra show absorption peaks of 1,2,4-trisubstituted benzene at 818 cm^{-1}, Si–CH_3 at 1251 cm^{-1}, 839 cm^{-1} and 794 cm^{-1}, and Si–O–Si at 1057 cm^{-1}. In addition, a broad absorption peak appeared in the range of 3400–2400 cm^{-1} for BZ-aptmds because of NH_2 and OH groups at the chain ends. ^1H NMR was employed to further prove the chemical structures of the three benzoxazine prepolymers (Fig. 2c; Fig. S1 and S2, ESI†). The typical peaks of the two protons on methylene (O–CH_2–N and Ar–CH_2–N) in the oxazine ring appear around 4.8 ppm (a) and 3.9 ppm (b), respectively. These two typical peaks of BZ-aptmds and CBZ-aptmds prepolymers appeared as multiples because of different chemical environments. The three polybenzoxazines have only one response peak in ^{29}Si NMR spectra (Fig. S3–S5, ESI†). The molecular weights of BZ-aptmds and CBZ-aptmds were characterized by GPC. Compared to BZ-aptmds, the weight average molecular weight (M_w) of CBZ-aptmds reduced from 3923 to 1743. In addition, the polydispersity index (PDI) of BZ-aptmds is 2.02, while that of CBZ-aptmds is 1.63. These results demonstrate that 4-cyclohexylphenol can not only effectively control the chain length of the main-chain benzoxazine but also narrow the distribution of molecular weight.

To understand the curing behavior of the obtained benzoxazine prepolymers, the DSC technique was employed to investigate their exothermic events. As shown in Fig. 2d, C-aptmds, BZ-aptmds, and CBZ-aptmds all exhibit an exothermic peak, and their peak temperatures (T_{peak}) are 237 °C, 198 °C, and 256 °C, respectively. Since BZ-aptmds has phenolic hydroxyl and amino groups at the chain end which could promote the ring-opening polymerization reaction as curing agents, the T_{peak} of BZ-aptmds is lower than that of the other two prepolymers. The obtained polybenzoxazines no longer exhibit exothermic events after undergoing the curing process, which proves that they have been fully cured. The structures of polybenzoxazines were characterized by FT-IR and the results are shown in Fig. 2e. A strong hydrogen bond peak appeared at 3416 cm^{-1} and the characteristic peaks of the benzoxazine ring at 941 and 923 cm^{-1} completely disappeared, both of which imply the occurrence of a ring-opening polymerization reaction. In addition, the absorption peaks of Si–O–Si at 1050 cm^{-1} and Si–CH_3 at 1253, 838, and 794 cm^{-1} hardly changed before and after curing. Fig. 3 shows the curing mechanism of benzoxazine C-aptmds. First, the C–O bond was broken and a carbocation was generated. Then, the electron-rich aromatic ring attacked the carbocation to form a cross-linked network. The curing mechanism of BZ-aptmds and CBZ-aptmds is similar to that of C-aptmds. The hydroxyl and amino groups at the chain end of BZ-aptmds can protonate the oxygen atom on the oxazine ring, which promotes the opening of the oxazine ring to form the carbocation. As a result, BZ-aptmds exhibits a relatively low T_{peak}.

2.2 Thermal properties of polybenzoxazines

Polybenzoxazines PC-aptmds, PBZ-aptmds, and PCBZ-aptmds were prepared according to the curing process described in section S1.5 of the ESI.† Their thermal stability properties were tested by TGA and the results are shown in Fig. 4a and Table S1 (ESI†). The three prepared polybenzoxazines all possess good thermal stability. The degradation temperatures at 10% mass loss ($T_{10\%}$) of PC-aptmds, PBZ-aptmds, and PCBZ-aptmds are 338 °C, 342 °C, and 344 °C, respectively. The char yield (CY) of main-chain PBZ-aptmds is appreciably higher than that of PC-aptmds because of the higher crosslink density.

DMA was applied to characterize the dynamic thermal-mechanical properties of the prepared polybenzoxazines. The curves of storage modulus (E') and Tan(δ) are shown in Fig. 4b. When the temperature is 30 °C, PBZ-aptmds has the highest E'

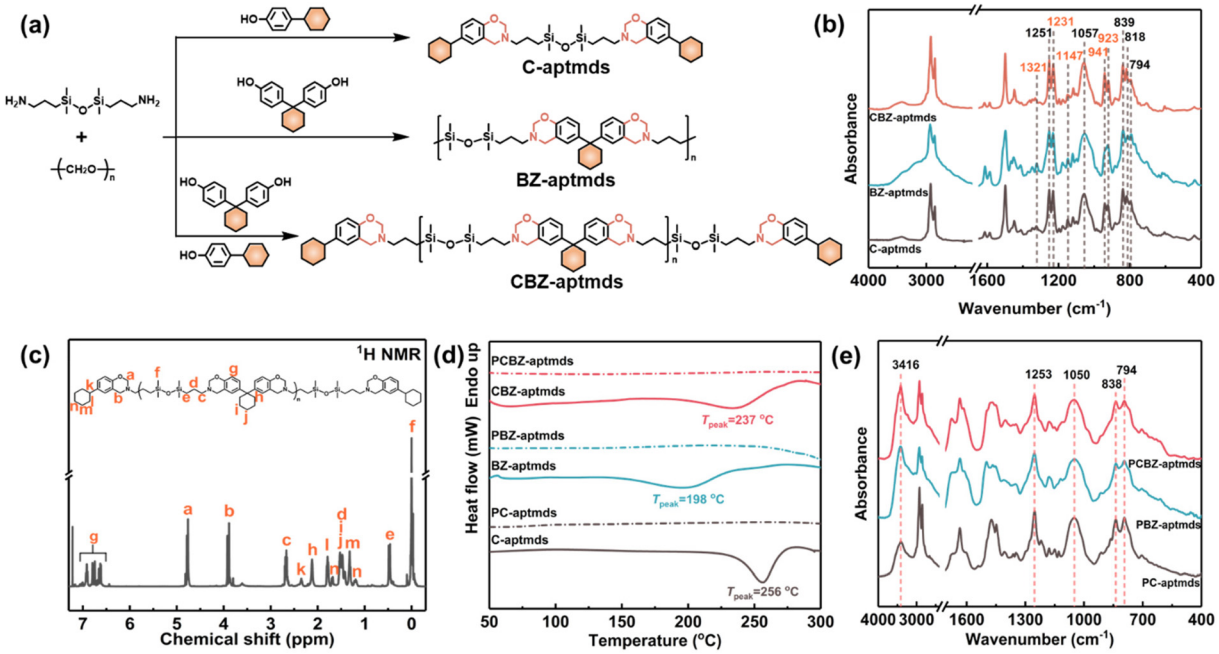

Fig. 2 Synthesis and characterization of benzoxazine prepolymers. (a) Synthesis routes to cyclohexyl-containing benzoxazine prepolymers C-aptmds, BZ-aptmds, and CBZ-aptmds. (b) FT-IR spectra of the three benzoxazine prepolymers. (c) ^{1}H NMR spectrum of CBZ-aptmds. (d) DSC curves of the three benzoxazine prepolymers and their corresponding polymers. (e) FT-IR spectra of the three polybenzoxazines.

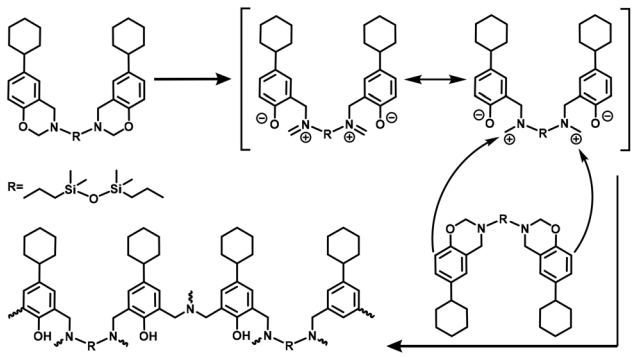

Fig. 3 Proposed curing mechanism of C-aptmds.

(3.8 GPa), followed by PCBZ-aptmds (3.0 GPa) and PC-aptmds (2.5 GPa). The peak temperature of Tan(δ) was recorded as the glass transition temperature (T_g). The E' and Tan(δ) of main-chain polybenzoxazine and the copolymer are enhanced to different degrees compared with those of bifunctional polybenzoxazine due to the positive effect of relatively high molecular weights. In addition, PC-aptmds and PCBZ-aptmds both show only one peak in the Tan(δ) curves, which proves that the microphase structures of the two polybenzoxazines are relatively uniform. Meanwhile, the Tan(δ) curve of PBZ-aptmds exhibits a broad peak, which implies that PBZ-aptmds has a different microphase structure due to the different molecular weight of main-chain BZ-aptmds.

The glass transition temperature could also be used to quantitatively characterize the crosslink density of polybenzoxazines according to eqn (1) and the results are listed in Table S1 (ESI†).

$$\log_{10}\left(\frac{E'_e}{3}\right) = 7.0 + 293(\rho_x) \quad (1)$$

where E'_e is the storage modulus (dyne per cm^2) at (T_g + 40) °C and ρ_x is the crosslink density (mol cm^{-3}). Bifunctional PC-aptmds has a ρ_x of 2.15 × 10^{-3} mol cm^{-3}, while main-chain PBZ-aptmds has an enhanced ρ_x of 2.99 × 10^{-3} mol cm^{-3}. The main-chain prepolymer has more crosslinking sites than the bifunctional benzoxazine monomer, and hence main-chain polybenzoxazine has a higher crosslink density.

Mean square displacement (MSD) can reflect the mobility of molecular chains quantitatively.[27] The MSD of the three polybenzoxazines was calculated by MD simulation of the NVT ensemble, and the results are shown in Fig. 4c. PBZ-aptmds consistently has the lowest MSD during the 10 ns simulation, which means that the molecular chains of PBZ-aptmds have the worst mobility among the three polybenzoxazines. The calculated results of MSD are consistent with the experimental results of DMA.

When the temperature is near T_g, the density of polymers will change obviously because of the recombination of the movement among molecular chains. Therefore, the inflection point in the density–temperature curve can simulate the glass transition process.[28] The three amorphous boxes of polybenzoxazines were cooled down from 550 K to 250 K at a rate of 20 K per 200 ps under 0.1 MPa. Fig. 4(d–f) show the density–temperature curves of PC-aptmds, PBZ-aptmds, and PCBZ-aptmds in order. The linear fitting was performed on the left

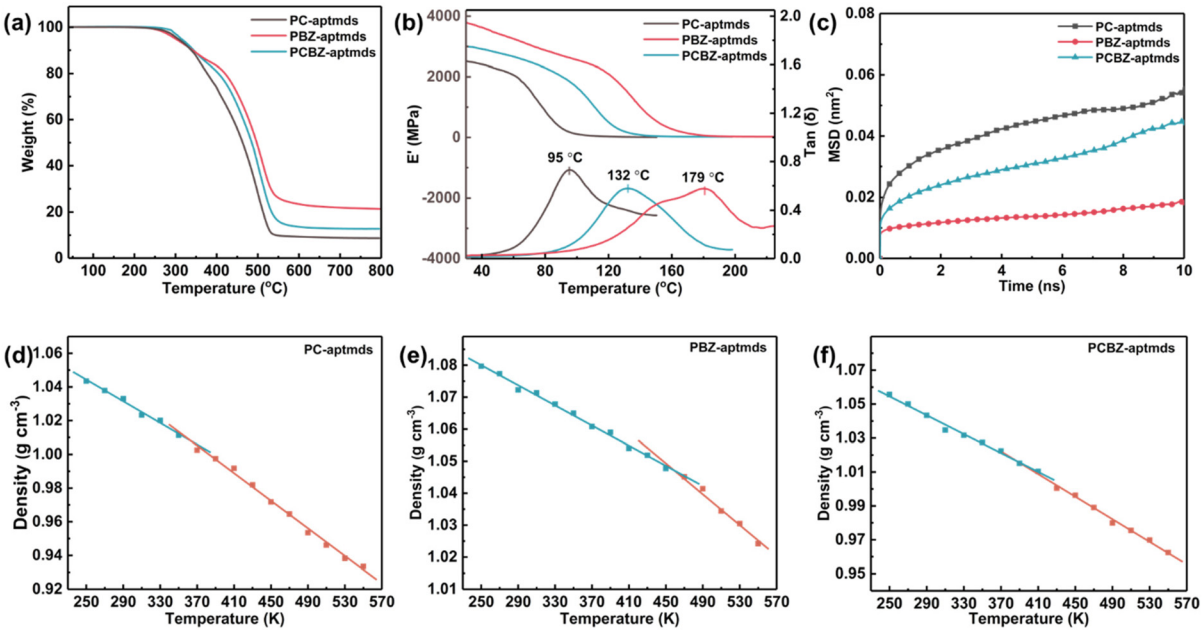

Fig. 4 Thermal stability and thermomechanical property characterization and simulation results of the three polybenzoxazines. (a) TGA curves, (b) DMA curves and (c) MSD curves of PC-aptmds, PBZ-aptmds, and PCBZ-aptmds. Density calculated at different temperatures and the corresponding linear regression curves of (d) PC-aptmds, (e) PBZ-aptmds and (f) PCBZ-aptmds.

and right sides of the inflection point. The temperatures corresponding to the intersection of the two fitting lines recorded as T_{gDFT} of PC-aptmds, PBZ-aptmds, and PCBZ-aptmds are 90 °C, 187 °C and 115 °C, respectively, which are close to the experimental values.

2.3 Wettability and dielectric properties of polybenzoxazines

Fig. 5a exhibits the surface morphology of polybenzoxazines. PC-aptmds and PCBZ-aptmds are both dark brown with poor transparency, while PBZ-aptmds is orange with better transpar-

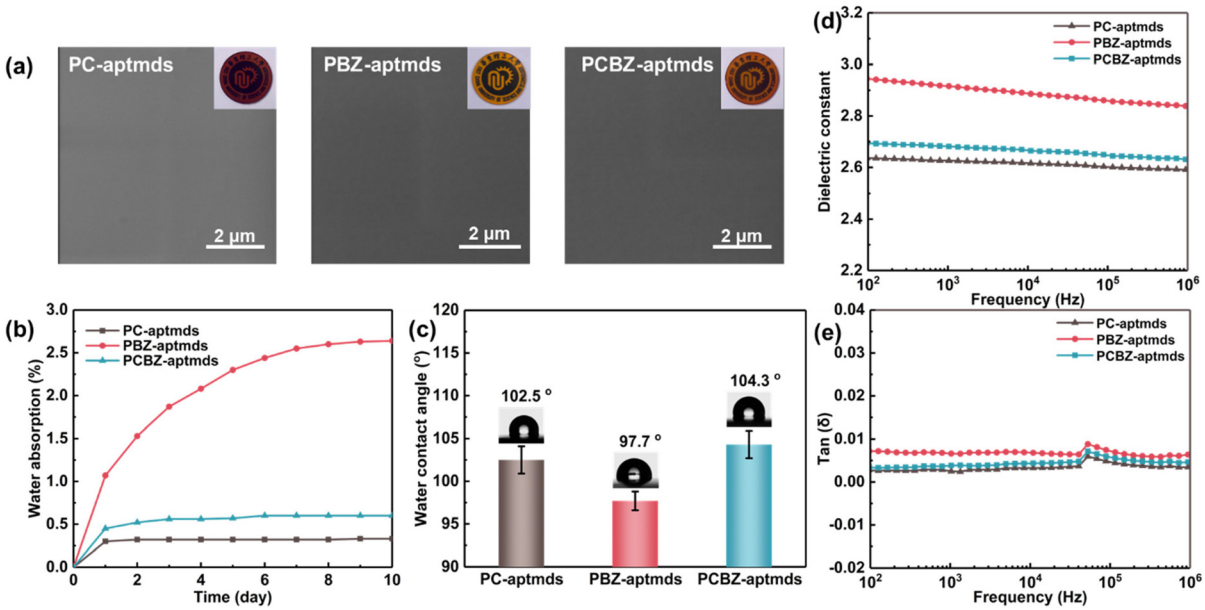

Fig. 5 Wettability and dielectric property characterizations of the three polybenzoxazines. (a) SEM images with a ruler of 2 μm and the corresponding macro morphology (inset images). (b) Water absorption of the three polybenzoxazines soaked in water for 10 days. (c) Static water contact angle of the three polybenzoxazines. (d) Dielectric constant and (e) dielectric loss tangent Tan(δ) of the three polybenzoxazines in the range of 100 Hz–1 MHz.

ency. The microscopic surface morphology of polybenzoxazines was observed by SEM. All three polybenzoxazines exhibit smooth surfaces without any defects, which proves that the three benzoxazine prepolymers all have superior film-forming properties.

It is well known that water has a high dielectric constant, for which reason dielectric materials should have good water repellency. Water absorption was tested by immersing polybenzoxazines in water for 10 days, and the results are shown in Fig. 5b. The water absorption of PC-aptmds and PCBZ-aptmds hardly changes after 2 days of immersion in water. After 8 days of immersion in water, the water absorption of PBZ-aptmds gradually reached the maximum. After 10 days of immersion, the water absorption of PC-aptmds, PBZ-aptmds, and PCBZ-aptmds is 0.33%, 2.64% and 0.60%, respectively. Due to the hydrophilicity of the polar groups at the chain end, PBZ-aptmds exhibits a relatively high water absorption. In addition, a water contact angle (WCA) test was performed to characterize hydrophobicity. As shown in Fig. 5c, PC-aptmds, PBZ-aptmds, and PCBZ-aptmds all exhibit hydrophobicity with WCAs of 102.5 ± 1.6°, 97.7 ± 1.1° and 104.3 ± 1.6°, respectively.

The dielectric properties of polybenzoxazines were measured from 100 Hz to 1 MHz at room temperature. As shown in Fig. 5d, all three polybenzoxazines have excellent frequency stability within the tested range. The main-chain polybenzoxazine PBZ-aptmds has the highest dielectric constant at all tested frequencies due to the polar groups exposed at the chain ends. The capping agent 4-cyclohexylphenol can react with the polar amino group at the end of the chain to form a oxazine ring. Therefore, PCBZ-aptmds fabricated with terminal oxazine rings has a dielectric constant close to that of PC-aptmds. The dielectric constants of PC-aptmds, PBZ-aptmds, and PCBZ-aptmds are 2.58, 2.83, and 2.62 at 1 MHz, respectively. C–C bonds in cyclohexane can lower the electron density and make the molecule difficult to polarize. In addition, cyclohexane can decrease the density of dipoles because of the large steric hindrance. Therefore, all three polybenzoxazines have a relatively low dielectric constant. The dielectric loss tangent Tan(δ) of the three polybenzoxazines was also investigated and the results are shown in Fig. 5e. Tan(δ) values of the three polybenzoxazines are 0.0032, 0.0067, and 0.0042, respectively, indicating their excellent dielectric loss performance for electronic applications.

2.4 Dielectric property simulation of polybenzoxazines

The surface electrostatic potentials (ESPs) of PC-aptmds, PBZ-aptmds, and PCBZ-aptmds repeat units were calculated by DFT, and the corresponding schematic diagrams are shown in Fig. 6a.[29,30] Compared to the other two polybenzoxazines, the ESP distribution of PC-aptmds is more even. To quantitatively compare the ESP distribution of the three polybenzoxazines, the area of different electronic potentials is shown in Fig. 6b. Generally, the wider the ESP distribution, the higher the polarity of the molecular segment. The region with |ESP| < 10 kcal mol^{-1} could be regarded as the non-polar domain.[23] The proportions of non-polar domains of PC-aptmds, PBZ-aptmds, and PCBZ-aptmds are calculated statistically to be 83.14%, 75.38%, and 76.95%, respectively. In addition, the proportions of regions with |ESP| > 20 kcal mol^{-1} of PC-aptmds, PBZ-aptmds, and PCBZ-aptmds are 3.01%, 6.60%, and 4.41%, respectively. Therefore, PC-aptmds with the highest proportion of non-polar domains has the weakest dipole polarization, followed by PCBZ-aptmds and PBZ-aptmds, respectively.

The polarizability which reflects the change of the dipole moment before and after applying one unit of electric field was calculated by the coupled-perturbed Kohn–Sham (CPKS) method. As shown in Fig. 6(c and d), α_{xx}, α_{yy}, and α_{zz} are the tensor components of polarizability, α_{iso} is the isotropic polarizability, and α_{aniso} is the anisotropy polarizability. The polarizability components of the three polybenzoxazines are similar, and the anisotropy polarizability of the three polybenzoxazines is relatively small, which indicates that all three polybenzoxazines have notable polarization isotropy. According to the theory proposed by Bader, the van der Waals volume V_{vdw} enclosed by an equivalent surface with an electron density of 0.002 a.u. was calculated.[31,32] Then, the volume polarizability α_{iso}/V_{vdw} of the three polybenzoxazines was calculated. Fig. 6e displays the correspondence between the dielectric constant at 1 MHz and volume polarizability of PC-aptmds, PBZ-aptmds, and PCBZ-aptmds, and linear regression analysis was performed. It was found that the dielectric constant highly correlates to the volume polarizability with a correlation coefficient of 0.94.

Furthermore, polarizability density analysis was employed to study the contribution of different regions of the molecular structure to polarizability.[33–35] Fig. 6f shows the polarizability density, namely $-z\rho_z^{(1)}$, of the three polybenzoxazines on the *YZ* plane, where red and blue regions denote positive and negative parts, respectively. It is obvious that PBZ-aptmds has the highest proportion of the red region, so PBZ-aptmds has the highest volume polarizability. The negative regions are predominantly present in the cyclohexyl and Si–O–Si chain regions, which indicates that the cyclohexyl and Si–O–Si chains are conducive to the reduction of polarizability. The contribution of each atom of the three polybenzoxazines obtained from lattice point integration to the polarizability is listed in Tables S2–S4 (ESI†). The molecular polarizability of polybenzoxazines calculated by the lattice point integration is similar to that obtained by the CPKS method, which further proves the reliability of the simulation results.

According to the Maxwell equation (eqn (2)), the dielectric constant at an infinite frequency (ε_∞) is equal to the square of the refractive index (n_D). Combining MD simulation and DFT simulation, n_D can be calculated using eqn (3) and (4), where N is the number density, α' is the polarizability volume calculated by DFT simulation, ρ is the mass density calculated by MD simulation, N_A is Avogadro's constant and M_{ru} is the molar mass of the repeat unit.[36] In addition, the static dielectric constant ε_s is computed as eqn (5), where T is the temperature, k_B

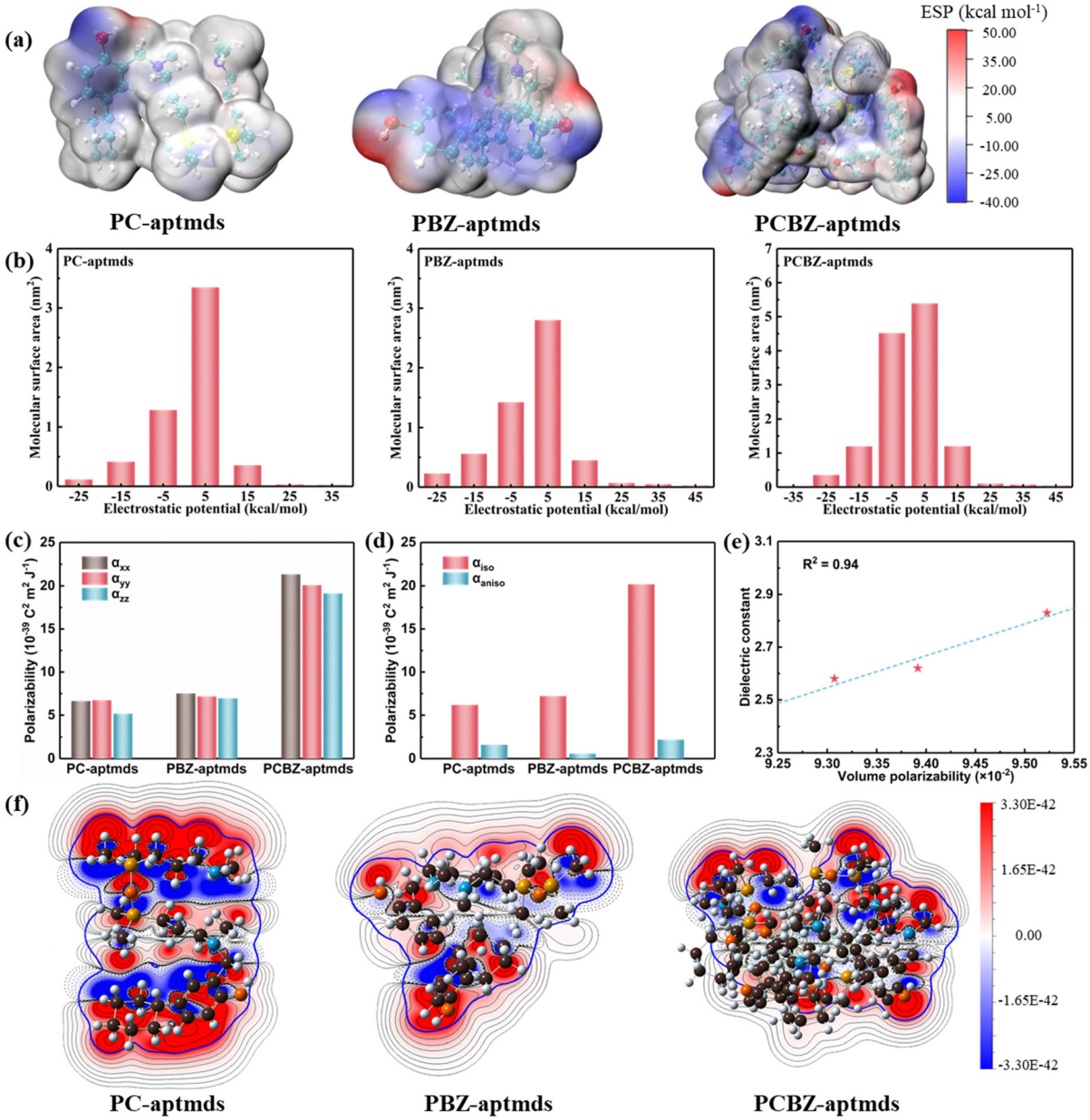

Fig. 6 DFT simulation of dielectric properties of polybenzoxazines. (a) Schematic diagram and (b) specific numerical distribution of surface electrostatic potential of the three polybenzoxazines. (c) Tensor components of polarizability of the three polybenzoxazines in the direction of *xx*, *yy* and *zz*. (d) Isotropic polarizability α_{iso} and anisotropic polarizability α_{aniso} of the three polybenzoxazines. (e) Correspondence of the dielectric constant at 1 MHz of the three polybenzoxazines and their volume polarizability, and the linear fitting curve. (f) Color-filled contour map of the integrand of $-z\rho_z^{(1)}$ on the *YZ* plane.

is Boltzmann's constant, and M is the dipole moment of the simulated box.[23,37,38]

$$\varepsilon_\infty = {n_D}^2 \quad (2)$$

$${n_D}^2 = 1 + \frac{4\pi N\alpha'}{1 - \frac{4}{3}\pi N\alpha'} \quad (3)$$

$$N = \frac{\rho N_A}{M_{ru}} \quad (4)$$

$$\varepsilon_s = \varepsilon_\infty + \frac{4\pi\langle M^2\rangle - \langle M^2\rangle}{3Vk_BT} \quad (5)$$

Table S5 (ESI†) summarizes the simulated numerical results and the experimental results of the dielectric constant. The density values of the three polybenzoxazines calculated by MD are in good agreement with these tested by the density balance, which proves that the simulated amorphous boxes are applicable. The static dielectric constant ε_s values of PC-aptmds, PBZ-aptmds, and PCBZ-aptmds are 2.90, 3.29, and

3.01, respectively, and the corresponding experimental values at 1 Hz are 2.66, 3.02, and 2.72, respectively. Generally, the dielectric constant decreases with increasing frequency, for which reason the dielectric constant at 1 Hz is smaller than ε_s. The simulation results and the experimental results have the same trend, indicating that this method is suitable for the prediction of the dielectric constant of polybenzoxazines.

3. Conclusions

In this work, novel cyclohexyl-containing polybenzoxazines with low dielectric constants, high hydrophobicity, and high thermal stability were prepared using a facile method. In particular, copolymer PCBZ-aptmds has a low dielectric constant of 2.62 and a low dielectric loss tangent of 0.0042 at 1 MHz. The relatively high crosslinking density endows PCBZ-aptmds with a high glass transition temperature of 132 °C and a high storage modulus of 3.0 GPa. In addition, PCBZ-aptmds absorbs only 0.44% of water after being immersed in water for 24 h. Furthermore, the dielectric constants of polybenzoxazines were simulated using MS and DFT, which were in high agreement with the corresponding experimental values. It is demonstrated that volume polarizability is an important factor influencing the dielectric constant of polybenzoxazines. Cyclohexyl and Si–O–Si chains with low polarizability endow PCBZ-aptmds with a low volume polarizability of 0.635. This method is suitable for guiding the design and development of low-*k* polybenzoxazines.

Author contributions

Manlin Yuan: conceptualization, methodology, validation, formal analysis, investigation, writing – original draft, and visualization. Xin Lu: resources, project administration, methodology, and writing – review and editing. Shiao-Wei Kuo: writing – review and editing. Zhong Xin: resources, supervision, writing – review and editing, and funding acquisition.

Conflicts of interest

There are no conflicts to declare.

Acknowledgements

This work was supported by the Innovation Program of the Shanghai Municipal Education Commission (2019-01-07-00-02-E00061) and the Shanghai Municipal Science and Technology Commission (21520761100).

References

1 W. Volksen, R. D. Miller and G. Dubois, *Chem. Rev.*, 2010, **110**, 56–110.
2 L. Wang, X. Liu, C. Liu, X. Zhou, C. Liu, M. Cheng, R. Wei and X. Liu, *Chem. Eng. J.*, 2020, **384**, 123231.
3 A. M. Evans, A. Giri, V. K. Sangwan, S. Xun, M. Bartnof, C. G. Torres-Castanedo, H. B. Balch, M. S. Rahn, N. P. Bradshaw, E. Vitaku, D. W. Burke, H. Li, M. J. Bedzyk, F. Wang, J. L. Bredas, J. A. Malen, A. J. H. McGaughey, M. C. Hersam, W. R. Dichtel and P. E. Hopkins, *Nat. Mater.*, 2021, **20**, 1142–1148.
4 S. Galli, A. Cimino, J. F. Ivy, C. Giacobbe, R. K. Arvapally, R. Vismara, S. Checchia, M. A. Rawshdeh, C. T. Cardenas, W. K. Yaseen, A. Maspero and M. A. Omary, *Adv. Funct. Mater.*, 2019, **29**, 1904707.
5 Y. Wang, W. Wu, D. Drummer, C. Liu, W. Shen, F. Tomiak, K. Schneider, X. Liu and Q. Chen, *Mater. Des.*, 2020, **191**, 108698.
6 Y. Lu, Y. Zhang and K. Zhang, *Chem. Eng. J.*, 2022, **448**, 137670.
7 C. J. Higginson, K. G. Malollari, Y. Xu, A. V. Kelleghan, N. G. Ricapito and P. B. Messersmith, *Angew. Chem., Int. Ed.*, 2019, **58**, 12271–12279.
8 M. Bai, J. Wang, R. Zhou, Z. Lu, L. Wang and X. Ning, *J. Hazard. Mater.*, 2022, **432**, 128735.
9 X. Fan, Z. Liu, J. Huang, D. Han, Z. Qiao, H. Liu, J. Du, H. Yan, Y. Ma, C. Zhang and Z. Wang, *Adv. Compos. Hybrid Mater.*, 2021, **5**, 322–334.
10 Y. X. Wang and H. Ishida, *Macromolecules*, 2000, **33**, 2839–2847.
11 K. Zhang, Q. Zhuang, X. Liu, G. Yang, R. Cai and Z. Han, *Macromolecules*, 2013, **46**, 2696–2704.
12 M. Yuan, X. Lu, Y. Zhao, S.-W. Kuo and Z. Xin, *Polymer*, 2022, **245**, 124572.
13 M. Zeng, D. Tan, Z. Feng, J. Chen, X. Lu, Y. Huang and Q. Xu, *Ind. Eng. Chem. Res.*, 2022, **61**, 115–129.
14 M. Zeng, J. Chen, Q. Xu, Y. Huang, Z. Feng and Y. Gu, *Polym. Chem.*, 2018, **9**, 2913–2925.
15 K. Zhang, X. Yu and S.-W. Kuo, *Polym. Chem.*, 2019, **10**, 2387–2396.
16 Y. Zhuang, R. Orita, E. Fujiwara, Y. Zhang and S. Ando, *Macromolecules*, 2019, **52**, 3813–3824.
17 L. Kong, Y. Cheng, Y. Jin, Z. Ren, Y. Li and F. Xiao, *J. Mater. Chem. C*, 2015, **3**, 3364–3370.
18 J. Zhu, M. Chu, Z. Chen, L. Wang, J. Lin and L. Du, *Chem. Mater.*, 2020, **32**, 4527–4535.
19 S. Han, Y. Li, F. Hao, H. Zhou, S. Qi, G. Tian and D. Wu, *Eur. Polym. J.*, 2021, **143**, 110206.
20 J. Wu, B. Wu, W. Wang, K. S. Chiang, A. K. Y. Jen and J. Luo, *Mater. Chem. Front.*, 2018, **2**, 901–909.
21 W. Zheng, T. Yang, L. Qu, X. Liang, C. Liu, C. Qian, T. Zhu, Z. Zhou, C. Liu, S. Liu, Z. Chi, J. Xu and Y. Zhang, *Chem. Eng. J.*, 2022, **436**, 135060.
22 J. Tong, Y. Huang, W. Liu, M. Shou, L. An, X. Jiang, P. Guo, Y. Han, Z. Liang, J. Li and Y. Xia, *J. Mater. Chem. C*, 2022, **10**, 16028.
23 K. Liu, H. Qin, M. Tian, L. Zhang and J. Mi, *Polymer*, 2022, **243**, 124657.
24 N. Jain and S. Thakur, *Macromolecules*, 2022, **55**, 2375–2382.

25 M. Misra, M. Agarwal, D. W. Sinkovits, S. K. Kumar, C. Wang, G. Pilania, R. Ramprasad, R. A. Weiss, X. Yuan and T. C. M. Chung, *Macromolecules*, 2014, **47**, 1122–1129.
26 Y. Tao, B. Yan, N. Zhang, M. Wang, J. Zhao, H. Zhang, W. Chen and D. Fan, *J. Food Eng.*, 2022, **316**, 110844.
27 J. Zhang, D. Wang, L. Wang, W. Zuo, L. Zhou, X. Hu and D. Bao, *Polymer*, 2021, **13**, 2451.
28 C. Li and A. Strachan, *Polymer*, 2010, **51**, 6058–6070.
29 T. Lu and F. Chen, *J. Comput. Chem.*, 2012, **33**, 580–592.
30 T. Lu and F. W. Chen, *J. Mol. Graphics Modell.*, 2012, **38**, 314–323.
31 R. F. W. Bader, M. T. Carroll, J. R. Cheeseman and C. Chang, *J. Am. Chem. Soc.*, 1987, **109**, 7968–7979.
32 Z. Y. Liu, T. Lu and Q. X. Chen, *Carbon*, 2021, **171**, 514–523.
33 Z. Liu, T. Lu and Q. Chen, *Carbon*, 2020, **165**, 461–467.
34 Z. Lin, T. Lu and X. L. Ding, *J. Comput. Chem.*, 2017, **38**, 1574–1582.
35 Z. Liu, Z. Tian, T. Lu and S. Hua, *J. Phys. Chem. A*, 2020, **124**, 5563–5569.
36 H. Lei, X. Li, J. Wang, Y. Song, G. Tian, M. Huang and D. Wu, *Chem. Phys. Lett.*, 2022, **786**, 139131.
37 N. Karasawa and W. A. Goddard III, *Macromolecules*, 1995, **28**, 6765–6772.
38 M. Misra, M. Agarwal, D. W. Sinkovits, S. K. Kumar, C. C. Wang, G. Pilania, R. Ramprasad, R. A. Weiss, X. P. Yuan and T. C. M. Chung, *Macromolecules*, 2014, **47**, 1122–1129.